$\mathcal{R}$esearch in
$\mathbf{A}$stronomy and
$\mathbf{A}$strophysics

A method of measuring the [α/Fe] ratios from the spectra of the LAMOST survey

Ji Li[1], Chen Han[1], Mao-Sheng Xiang[2,3], Jian-Rong Shi[3], Jing-Kun Zhao[3], Xiao-Wei Liu[2,4],

Hua-Wei Zhang[2,4], Hai-Bo Yuan[2,5], Xuan Ci[1], Xiao-Feng Zhang[1], Yue-Xiang Wang[1], Yang Huang[2],

Yong Zhang[6], Yong-Hui Hou[6], Yue-Fei Wang[6], Zi-Huang Cao[3]

[1] Department of Space Science and Astronomy, Hebei Normal University, Shijiazhuang 050024, China; *liji@hebtu.edu.cn*
[2] Department of Astronomy, Peking University, Beijing 100871, China
[3] Key Laboratory of Optical Astronomy, National Astronomical Observatories, Chinese Academy of Sciences, Beijing 100012, China
[4] Kavli Institute for Astronomy and Astrophysics, Peking University, Beijing 100871, China
[5] Department of Astronomy, Beijing Normal University, Beijing 100875, China
[6] Nanjing Institute of Astronomical Optics & Technology, National Astronomical Observatories, Chinese Academy of Sciences, Nanjing 210042, China

Abstract   The [α/Fe] ratios in stars are good tracers to probe the formation history of stellar populations and the chemical evolution of the Galaxy. The spectroscopic survey of LAMOST provides a good opportunity to determine [α/Fe] of millions of stars in the Galaxy. We present a method of measuring the [α/Fe] ratios from LAMOST spectra using the template-matching technique of the LSP3 pipeline. We use three test samples of stars selected from the ELODIE and MILES libraries, as well as the LEGUE survey to validate our method. Based on the test results, we conclude that our method is valid for measuring [α/Fe] from low-resolution spectra acquired by the LAMOST survey. Within the range of the stellar parameters $T_{\rm eff} = [5000, 7500]$ K, $\log g = [1.0, 5.0]$ dex and [Fe/H]$= [-1.5, +0.5]$ dex, our [α/Fe] measurements are consistent with values derived from high-resolution spectra, and the accuracy of our [α/Fe] measurements from LAMOST spectra is better than 0.1 dex with spectral signal-to-noise higher than 20.

Key words: Galaxy: evolution — stars: abundances — stars: fundamental parameters — techniques: spectroscopy surveys — methods: data analysis

1 INTRODUCTION

According to the theory of nucleosynthesis (Burbidge et al. 1957), it is believed that all of the H, a major part of He and some Li were produced during the Big Bang, whereas the heavier elements are thought to be produced in stars. In fact, the chemical composition in the atmospheres of main sequence stars represents the chemical composition of the interstellar medium from which the stars were formed, so that the abundances of elements in stars provide the main observational evidence for the formation of stars and the chemical evolution of the Galaxy. In this context, the stellar abundance ratios of α-elements to iron [α/Fe] are particularly useful due to their unique characteristics. In the framework of standard nucleosynthesis, the α-elements, such as Mg, Si, Ca and Ti, are mainly produced by successive capture of α-particles in massive stars and dispersed into the interstellar medium by type II supernovae (SNe)

explosions on a timescale of $\sim 10^7$ years, whereas the bulk of Fe is produced by type Ia SNe on a much longer timescale of $\sim 10^9$ years (Tinsley 1979; McWilliam 1997). Therefore, the [α/Fe] ratios can be used as a cosmic clock to trace the history of the chemical evolution of the Galaxy. On the other hand, observational studies have found that the abundances of [α/Fe] are distinct in different stellar populations. The thick disk population generally shows higher [α/Fe] ratios than the thin disk (Fuhrmann 2004; Bensby et al. 2004). Moreover, the halo stars in the solar neighborhood are found to be divided into two populations, clearly separated in [α/Fe], called the "low-α" and "high-α" halo stars (Nissen & Schuster 2010). These observations imply that the [α/Fe] ratios can be used as stellar population tracers. Thus the [α/Fe] ratios in a large number of stars not only provide constraints on the models of chemical evolution of the Galaxy, but can also be used to disentangle various stellar populations in the Galaxy.

To measure precise elemental abundances in stellar atmospheres, the ideal method is to measure the equivalent widths of the spectral lines of each element using high resolution ($R > 30\,000$) and high signal-to-noise ratio (SNR > 100) stellar spectra. At present, most observations of [α/Fe] are derived from high-resolution stellar spectra (e.g., Edvardsson et al. 1993; Chen et al. 2000; Fulbright 2002; Gratton et al. 2003; Fuhrmann 2004; Soubiran & Girard 2005; Zhang & Zhao 2006; Reddy et al. 2006; Bensby et al. 2014; Adibekyan et al. 2013). However, in order to obtain high-quality spectra, the sample stars in these observations are usually restricted to be in the solar neighborhood and are limited in number to several hundred at most. Moreover, different studies often adopt different stellar atmosphere models, atomic line data and analysis methods. Consequently, individual studies inevitably suffer from some selection effects due to the small number of stars, and it is very cumbersome to compose a unified view of the chemical evolution of the Galaxy from various observations. In order to avoid the sample selection effects, we should turn to use low-resolution stellar spectra to obtain the [α/Fe] ratios for a great number of stars. Fortunately, a number of low-to-medium resolution spectroscopic surveys have been undertaken to obtain stellar spectra for sample sizes ranging from $\sim 10^4$ to $\sim 10^7$ stars, such as the Radial Velocity Experiment (RAVE; Steinmetz et al. 2006), the Sloan Extension for Galactic Understanding and Exploration (SEGUE; Yanny et al. 2009), and the Large Sky Area Multi-Object Fiber Spectroscopic Telescope (LAMOST) Experiment for Galactic Understanding and Exploration (LEGUE; Zhao et al. 2012; Deng et al. 2012), etc.

The LEGUE survey is the main project of the LAMOST spectroscopic survey, which consists of three parts including the LAMOST Spectroscopic Survey of the Galactic Anti-center (LSS-GAC; Liu et al. 2014; Yuan et al. 2015), the Galactic disk survey and the Galactic halo survey; one can see a detailed description of the LEGUE survey in Deng et al. (2012). According to the science plan of the LAMOST survey, within five years starting from the fall of 2012, LAMOST will observe at least 2.5 million stars in a contiguous area in the Galactic halo, and more than 7.5 million stars in low Galactic latitude areas around the plane (Zhao et al. 2012). Up to 2015 May 30, the data release (DR) of LAMOST includes the pilot survey and three years regular survey. DR1, DR2 and DR3 have at present a total of 5 268 687 stellar spectra as reported on the LAMOST website[1]. With such a huge sample of stars, we can obtain detailed abundances of [α/Fe] to study the chemical evolution and stellar populations of our Galaxy by constructing a complete sample in space.

LAMOST spectra are low-resolution spectra with $R \sim 1800$ in a wavelength range of 3690–9100 Å (Luo et al. 2015), and for such spectra, it is very difficult to define a reliable continuum and measure equivalent widths of weak spectral lines of the α-elements. At present, there are two ways to derive the abundance ratios from low-resolution spectra: one is fitting a synthetic spectral line profile calculated from a model atmosphere to the observed line profile of a target by taking the abundance of [α/Fe] as a free parameter (e.g., Lee et al. 2011); the other is using the line-indices that can be calibrated via high-resolution data or by model-atmosphere calculations (e.g., Franchini et al. 2010, 2011). Lee et al. have developed the SEGUE Stellar Parameter Pipeline (SSPP; Lee et al. 2008, 2013) to derive [α/Fe] from the spectra of the SDSS/SEGUE survey. For the LEGUE survey, Xiang et al. (2015) have developed the LAMOST Stellar Parameter Pipeline at Peking University (LSP3 hereafter) to derive the stellar atmospheric parameters from spectra of the LSS-GAC survey. In this work, we extend the function of LSP3 and develop a technique for measuring the [α/Fe] ratios from LAMOST spectra. Section 2 describes the details of the technique and the process of determination, and Section 3 presents three validation exercises for our method. Section 4 provides the uncertainties in our [α/Fe] measurements, and Section 5 describes the factors that impact the resulting uncertainties in our [α/Fe] measurements. The summary is given in Section 6.

2 METHODOLOGY

We derive the [α/Fe] ratios from the LAMOST spectra using the template matching method by means of the LSP3. Such a method requires a set of synthetic spectra as the template spectra with various atmospheric parameters ($T_{\rm eff}, \log g$, [Fe/H] and [α/Fe]) to match the observed stellar spectra.

2.1 Grid of Synthetic Spectra

Our synthetic spectra are created based on the stellar atmosphere models of Kurucz ODFNEW (Castelli & Kurucz 2004) using the SPECTRUM synthesis code (V2.76, 2010). The ODFNEW atmospheric models employ solar abundances of Grevesse & Sauval (1998) with no enhancements of α-element abundances. To generate the synthetic grid of [α/Fe], we change the abundances for each of the α-elements (Mg, Si, Ca and Ti) by the same amount. In the process of spectral synthesis, we have included contributions from the isotopes of magnesium to generate a reasonable synthetic profile for the $\lambda\lambda$5168, 5183 Å Mg I b lines. We adopt a microturbulence of 2.0 km s^{-1} for all spectra. The calculated synthetic spectra have a step of 0.1 Å in wavelength, and we bin them into 1 Å per pixel for template matching. In order to match with the non-normalized LAMOST spectra, we adopt the non-normalized specific intensity spectrum as the output of SPECTRUM.

Based on the original grid of KURUCZ ODFNEW models and linearly interpolating the original grids, we generate a finer grid of synthetic spectra with ranges of atmospheric parameters: $4000\,{\rm K} \leq T_{\rm eff} \leq 8000\,{\rm K}$ in steps of 100 K, $0.0 \leq \log g \leq 5.0$ in steps of 0.25 dex, $-4.0 \leq$ [Fe/H] ≤ -1.0 in steps of 0.2 dex, $-1.0 <$ [Fe/H] ≤ 0.5

in steps of 0.1 dex and $-0.4 \leq$ [α/Fe] ≤ 1.0 in steps of 0.2 dex.

2.2 Determination of [α/Fe]

To make a pixel to pixel match between the synthetic and observed spectra, some preprocessing of the synthetic and observed spectra needs to be done before spectral matching. First, the synthetic spectra must be degraded to the mean resolution of the LAMOST spectra ($R = 1800$) using a Gaussian kernel and re-sampling them to 1 Å per pixel in the spectral range 3670 – 6800 Å to match the LAMOST spectra which have been linearly re-binned to 1 Å per pixel. Second, the wavelength scale of the observed spectra need to be converted from vacuum-based to air-based after being corrected by the radial velocity (V_r).

In order to determine the overall behavior of the four α-elements (Mg, Si, Ca and Ti), we choose two spectral ranges 4400 – 4600 Å and 5000 – 5300 Å, in which there are a few prominent lines of Mg I, Ti I and Ca I. These lines are very sensitive to the α-abundances as shown in Figure 1. Compared with the wavelength ranges used by Lee et al. (2011), we use the spectral band 4400 – 4600 Å instead of their 4500 – 4580 Å and thus add three spectral lines of Ca I, Ti I and Ti II. We need to note that measurement of the [α/Fe] ratio is in fact the unweighted average abundance ratios of the four α-elements, since we have assumed that their abundances vary by the same amount when generating the synthetic spectra.

The LSP3 follows two stepwise approaches to estimate the [α/Fe] ratios from low-resolution spectra. First, it generates a set of template spectra by inputting the atmospheric parameters (T_{eff}, $\log g$ and [Fe/H]) of one star but with different values of [α/Fe] from -0.4 dex to 1.0 dex in steps of 0.2 dex. As a result, we get eight template spectra with different [α/Fe] values for one observed stellar spectrum. This calculation is an iterative process using the interpolation method between the different grids of synthetic spectra. To examine the uncertainties of the interpolated template spectra, we applied an interpolation scheme to the synthetic grids themselves. Specifically, we remove a spectrum from the grids of synthetic spectra, and then calculate a template with the same fundamental atmospheric parameters and [α/Fe] of the removed spectrum using the interpolation scheme. To characterize the accuracy of the interpolation, the dispersion of the relative differences between the interpolated and original synthetic spectra is calculated between 5000 and 5500 Å, which covers the main window we adopt for [α/Fe] estimation (see Fig. 2). We find that the interpolated spectrum is very consistent with the original synthetic spectrum, and the small dispersion can be ignored compared with the uncertainties induced by uncertainties in the fundamental atmospheric parameters (see, e.g., Xiang et al. 2015) and uncertainties of the target spectra. This test indicates our interpolation algorithm is reliable and accurate.

The second step is to search for the best match between the template and the observed spectra using a χ^2 minimization routine. The χ^2 is defined as

$$\chi^2 = \sum_{i=1}^{N} \frac{(O_i - T_i)^2}{\sigma_i^2}, \qquad (1)$$

where O_i and T_i are the flux of the observed and template spectra at the i_{th} pixel respectively. σ_i is the flux error of the observed spectra at the i_{th} pixel, and N is the total number of pixels used to calculate the χ^2 over the wavelength ranges of 4400 – 4600 Å and 5000 – 5300 Å. Previous work usually normalized the spectra with a fitted continuum for template matching (e.g. SSPP; Lee et al. 2011). However, considering that a large fraction of LAMOST spectra have pixel SNR at the blue setting (3800 – 6000 Å) lower than 20, and there are also many late-type stars designed in the survey of LSS-GAC (Yuan et al. 2015), it is difficult to obtain an accurate global continuum within a wide wavelength range. LSP3 thus has opted to not normalize the spectra but match the continuum-characterized target spectra with templates directly. Considering the fact that an observed stellar spectrum is not only determined by the stellar atmospheric parameters, but also affected by other processes, like interstellar extinction and flux calibration (Xiang et al. 2015), we adopt a third-order polynomial correction for the difference in spectral shape between the target spectra and the templates when calculating the χ^2. Finally, the calculated χ^2 values are fitted with a Gaussian plus second-order polynomial to determine the minimum value of χ^2, and its corresponding [α/Fe] value is the measurement of [α/Fe] by the LSP3.

Figure 3 shows the fitting results for two sample stars from the LSS-GAC survey as examples of spectral matching. The left plot shows a star with $T_{eff} = 5865$ K, $\log g = 4.22$, [Fe/H]=0.09 and [α/Fe]=0.02, while the right plot shows a metal-poor star with $T_{eff} = 6107$ K, $\log g = 4.18$, [Fe/H] $= -1.65$ and [α/Fe] $= 0.19$. The solid line (black) is the observed spectrum, while the dashed line (red) is the template spectrum generated with the corresponding fundamental atmospheric parameters and the [α/Fe] listed in each plot. The bottom panels of each plot show the distribution of residuals, from which we note that most of the deviations between the observed and template spectra are no more than a few percent for the two examples; even the largest deviation is no more than ten percent. Such a small deviation means that the synthetic and observed spectra achieved an excellent match for the two sample stars.

3 VALIDATION OF THE METHOD

In order to verify the validation of our method in measuring [α/Fe] from low-resolution spectra, and quantify possible systematic offsets of the [α/Fe] measurements, the ideal way is to compare the [α/Fe] estimates star by star against different sources. For these purposes, we apply our method to three different samples: 425 spectra of 293 sample stars
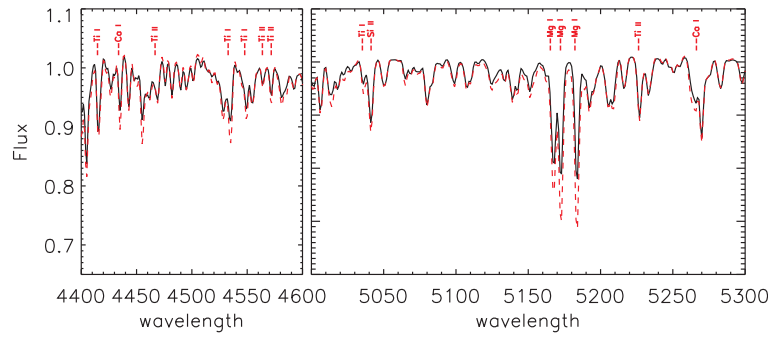
Fig. 1 The spectral wavelength ranges and the spectral features used to determine [α/Fe]. The black solid and red dashed lines represent a synthetic spectrum with the same atmospheric parameters of $T_{\rm eff} = 5500$ K, $\log g = 4.5$, [Fe/H]$= -1.4$, but with different [α/Fe] of 0 and 0.4, respectively.
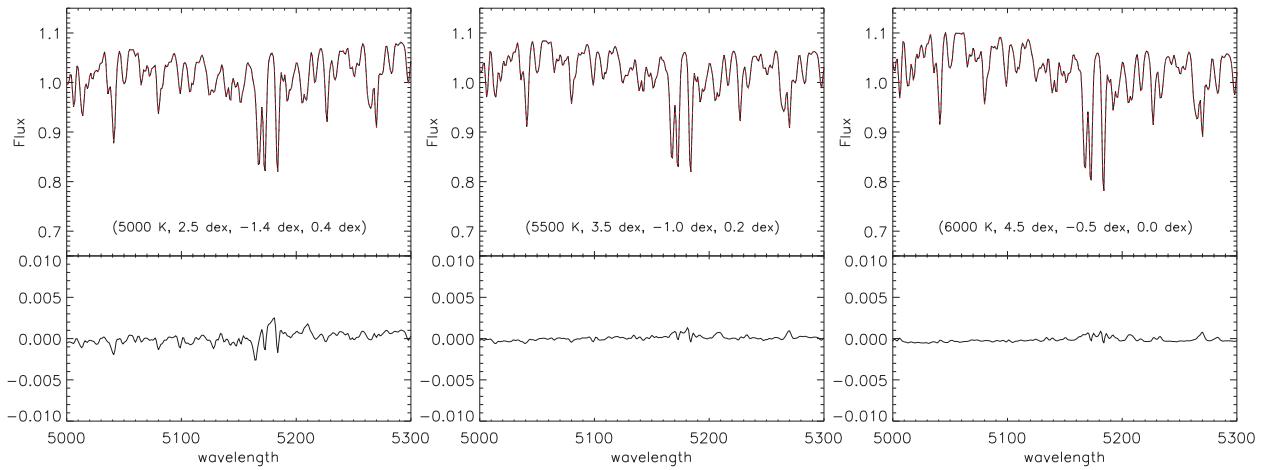

Fig. 2 Comparison of an interpolated synthetic spectrum (*red dashed line*) with its counterpart, the original synthetic spectrum (*black solid line*), for three cases. The atmospheric parameters (in the sequence of $T_{\rm eff}$, $\log g$, [Fe/H] and [α/Fe]) of the spectrum are marked in each panel, and the residuals of the interpolated values minus the synthetic spectrum are plotted at the bottom of each panel.
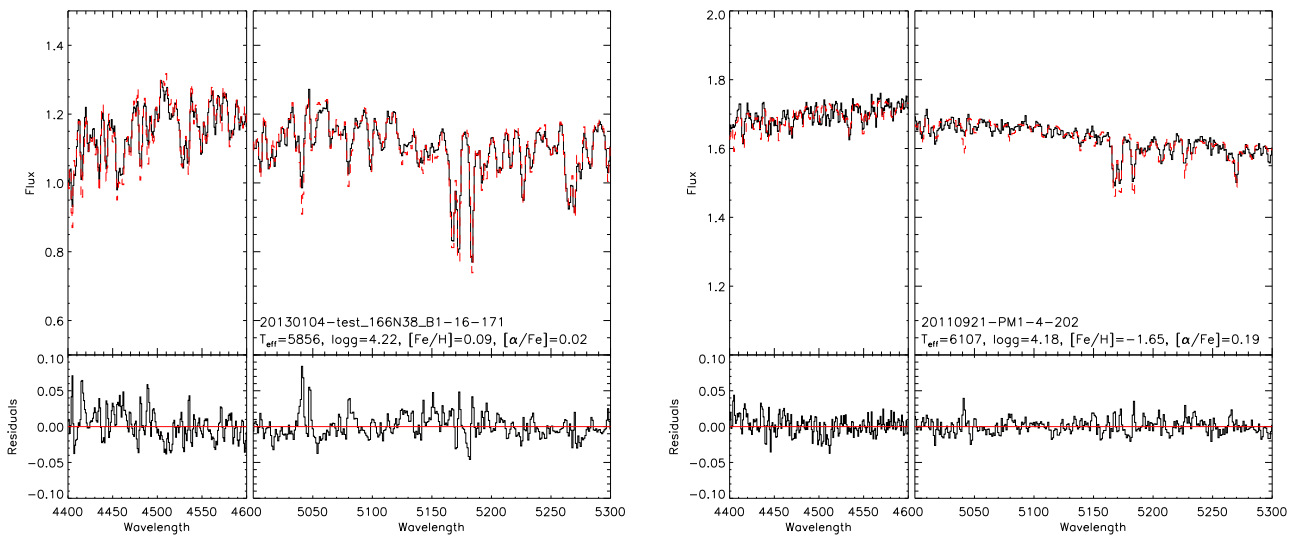
Fig. 3 The fitting results for two sample stars from the LSS-GAC survey as examples of spectral matching. The solid line (*black*) is the observed spectrum, while the dashed line (*red*) is the template spectrum. The bottom panels plot the residuals of the spectral matching.

from the ELODIE (Prugniel et al. 2007) spectral library, 177 stellar spectra from the MILES (Sánchez-Blázquez et al. 2006; Falcón-Barroso et al. 2011) spectral library and 98 stellar spectra from the LEGUE survey.

3.1 Testing with the ELODIE Spectra

The ELODIE library (Prugniel et al. 2007) contains 1962 spectra of 1388 stars (version ELODIE 3.1; Moultaka et al. 2004). The ELODIE spectra are presented with two different spectral resolutions ($R = 42\,000$ and $R = 10\,000$) and high SNR (SNR>100) over the wavelength coverage 3900–6800 Å. Due to its large coverage in atmospheric parameters, the ELODIE library is widely used as a reference sample for the automatic determination of stellar atmospheric parameters (e.g., Wu et al. 2011 and Xiang et al. 2015). Although the ELODIE catalog does not provide [α/Fe] measurements, they are available from a literature search via the VizieR database. Thus, we can employ the ELODIE library to validate our method by comparing the LSP3 [α/Fe] measurements with the values derived from high-resolution spectra in the literature. Lee et al. (2011) have compiled a sample of 293 stars from the ELODIE catalog to validate the SSPP method for measuring [α/Fe] from the SEGUE spectra. Their table 1 listed the atmospheric parameters $T_{\rm eff}$, $\log g$ and [Fe/H] from the ELODIE catalog, and the [α/Fe] values from the literature were searched with the VizieR database. Figure 4 shows the space of atmospheric parameters for the 293 ELODIE sample stars and the distribution of [α/Fe] along with [Fe/H].

In our test we choose the same sample of stars as Lee et al. (2011) used. In order to evaluate the uncertainty in the [α/Fe] measurements that resulted from the LSP3 alone, we adopt the atmospheric parameters from the ELODIE catalog instead of values determined with the LSP3 pipeline to ensure no errors are added to the [α/Fe] measurements from the fundamental atmospheric parameters. Since some sample stars in the ELODIE library were observed multiple times, there are 425 spectra for the 293 sample stars in this test. These stellar spectra should be degraded to the synthetic spectral resolution of $R =1800$ and re-sampled to 1 Å per pixel in the wavelength range 4300 – 5400 Å. Then the [α/Fe] ratios of the sample stars are determined with the LSP3 pipeline by feeding both the spectra of sample stars and the synthetic spectra.

The left panel of Figure 5 shows the comparison of [α/Fe] ratios between the measurements of LSP3 and the values from the literature for the ELODIE sample stars, while the right panel shows that there is an overall offset of -0.125 dex between our measurements and values of [α/Fe] from the literature, along with a dispersion of 0.071 dex. Similarly, nearly the same offset also appears in the following comparisons for the samples of the MILES library and the LEGUE survey (see Sect. 3.2 and 3.3 below). Is it a universal offset for the [α/Fe] measurements determined by template-matching compared with the high-

resolution spectroscopic analysis? Lee et al. (2011) also find that it requires a zero point offset of 0.13 dex for the [α/Fe] measurements from the SEGUE spectra using SSPP to force [α/Fe]= 0 at [Fe/H]= 0 and to agree with the measurements derived from the high-resolution spectra. It means that there is a systemic offset of -0.13 dex for the [α/Fe] measurements of SSPP compared to the values from high-resolution spectra. Boeche et al. (2011) measured [α/Fe] from the medium-resolution spectra of the RAVE survey using the RAVE pipeline. They found that their [α/Fe] measurements show a systematically lower offset of -0.11 dex compared with the values derived from high-resolution spectroscopic analysis in the literature (Soubiran & Girard 2005).

From the results of comparisons for our three test samples, we find a nearly uniform systematic deviation of about -0.13 dex in our [α/Fe] measurements. Thus, we take this systematic deviation of -0.13 dex as the zero-point offset for our [α/Fe] measurements, and the dashed line in the left panel of Figure 5 gives the one-to-one comparison after being corrected by the zero-point offset. To keep internal consistency with our measurements of [α/Fe], we apply the same offset to the following two test samples in Sections 3.2 and 3.3. Figure 6 displays the distributions of the differences of [α/Fe] between the LSP3 measurements and the literature values as a function of the atmospheric parameters $T_{\rm eff}$, $\log g$ and [Fe/H] from the upper to lower panels respectively. It shows there are no clear correlations between the [α/Fe] differences with the $T_{\rm eff}$, $\log g$ and [Fe/H], but a small increasing trend appears for cold stars with $T_{\rm eff} < 5500$ K.

3.2 Testing with the MILES Spectra

The MILES library provides the spectra of 985 stars, covering the wavelength range 3525 – 7500 Å (Sánchez-Blázquez et al. 2006). The spectral resolution is 2.5 Å in terms of full width at half maximum (FWHM) (Falcón-Barroso et al. 2011). By cross-matching the MILES library with the catalog of Soubiran & Girard (2005), we obtain a sample of 177 MILES stars with 'known' [α/Fe] values from the literature of high-resolution spectroscopic analysis. The distributions of the 177 stars in parameter space are shown in Figure 7.

After degrading the MILES spectra to the synthetic spectral resolution of 2.8 Å FWHM and re-sampling to 1 Å per pixel, we determine the [α/Fe] of the 177 selected MILES stars by the LSP3 pipeline, adopting the fundamental atmospheric parameters from the MILES library. Figure 8 plots the comparison of [α/Fe] ratios between our measurements and the values in the literature of high-resolution spectroscopic analysis (left panel), as well as a Gaussian fit for the differences (right panel). The right panel of Figure 8 exhibits a systematic deviation of -0.148 dex with a difference dispersion of 0.085 dex between LSP3 measurements and the values from the literature. Considering the zero-point offset of -0.13 dex (we
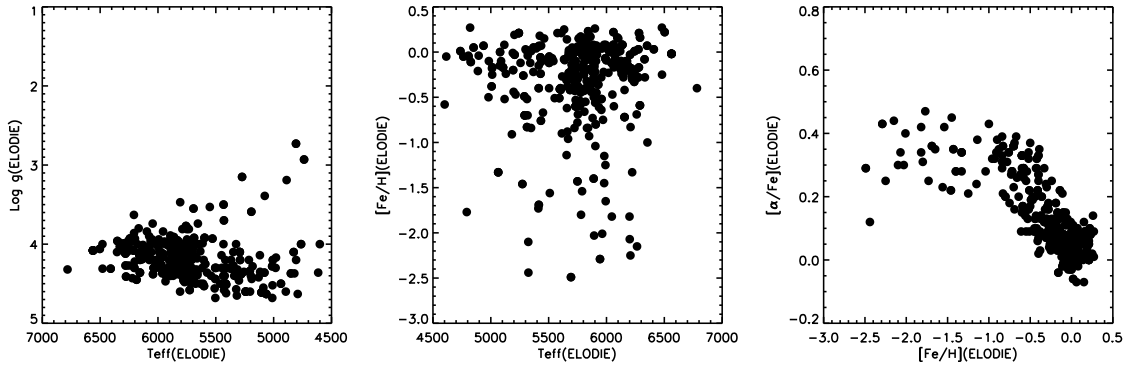
Fig. 4 Distribution of the ELODIE sample in $T_{\rm eff} - \log g$, $T_{\rm eff}$–[Fe/H] and [α/Fe] – [Fe/H] space.
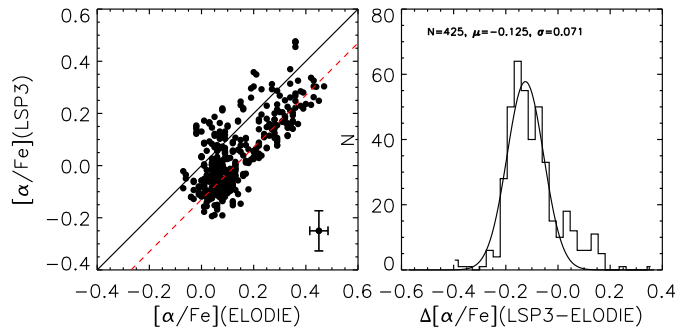

Fig. 5 Comparison of [α/Fe] between measurements of LSP3 and values from the literature for the ELODIE sample stars. "ELODIE" denotes [α/Fe] from the literature, while "LSP3" denotes our measurements using LSP3. The left panel plots our measurements against the literature values. The solid and dashed lines show the true one-to-one correspondence and that after zero-point correction via an overall shift of 0.13 dex, respectively. The right panel is a Gaussian fit to the differences between our measurements and those from the literature.

have set for the LSP3 measurements in Sect. 3.1), such a systematic deviation will decrease to -0.018 dex, which is much less than the errors that result from the stellar atmospheric parameters (cf. Sect. 5.1). Figure 9 displays the distributions of [α/Fe] differences alone with the atmospheric parameters $T_{\rm eff}$, $\log g$ and [Fe/H] from upper to lower panels respectively. Figure 9 shows that the deviations vary around zero with no trends over the whole range of atmospheric parameters, which means that the LSP3 [α/Fe] measurements for the MILES sample stars have no obvious correlation with any of the atmospheric parameters.

3.3 Testing with the LEGUE Spectra

Our method estimates [α/Fe] from LAMOST spectra, thus the optimal test comes from a comparison of the [α/Fe] measurements from LAMOST spectra with values from high-resolution spectral analysis for the same sample of stars. By cross-matching the LAMOST DR1 (Luo et al. 2015) with the PASTEL catalog (Soubiran et al. 2010) and Hypatia catalog (Hinkel et al. 2014), we obtained a sample suitable for such a comparison. PASTEL is an [Fe/H] catalog and also provides stellar atmospheric pa-

rameters of about 6000 stars derived from the analysis of high resolution, high SNR spectra, carried out with model atmospheres. The Hypatia catalog compiles spectroscopic abundance data from 84 literature sources for 50 elements for 3058 stars in the solar neighborhood, within 150 pc from the Sun. We obtained a sample of 130 common stars by cross-matching the catalog of LAMOST DR1 with the catalogs of PASTEL and Hyoatia, and the [α/Fe] values based on high-resolution spectroscopic analysis are searched from the VizieR database. Because some stars have no available LAMOST stellar parameters, the final sample contains 98 unique stars with spectral SNR higher than 30. For convenience, this sample is named the high-resolution sample (HRS) hereafter.

The stellar parameters of the HRS stars are obtained by the LSP3 (Xiang et al. 2015) and most of them have been collected in the first DR of value-added catalogs of LSS-GAC (Yuan et al. 2015). Table 1 lists the atmospheric parameters and the [α/Fe] values from the literature and the LSP3 measurements for HRS stars. The distributions in stellar atmospheric parameter space of the HRS stars are shown in Figure 10. Although the number of HRS stars is relatively small at present, it shows that the stellar atmo-
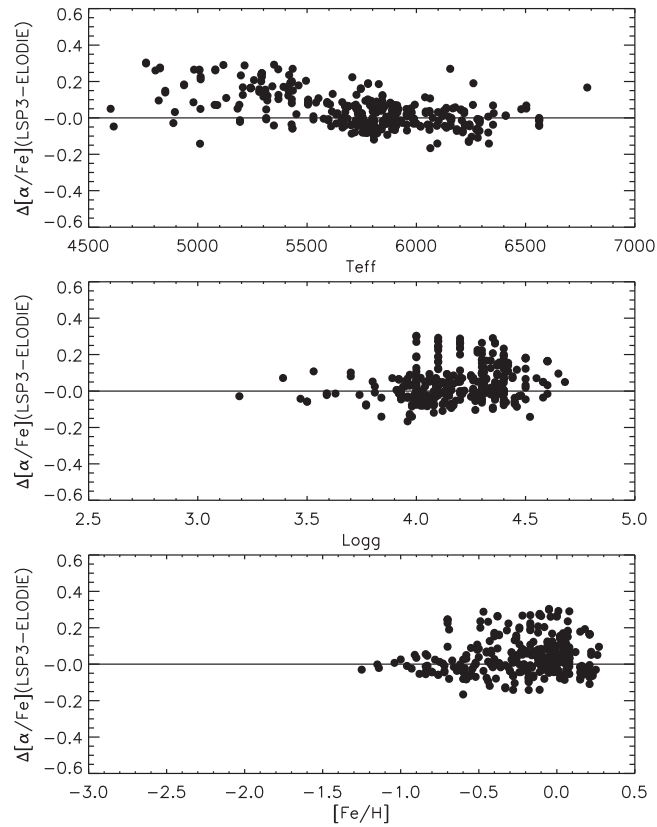
Fig. 6 The differences of [α/Fe] between the LSP3 measurements and high-resolution values as functions of $T_{\rm eff}$ (*top*), $\log g$ (*middle*) and [Fe/H] (*bottom*), for the ELODIE stars.
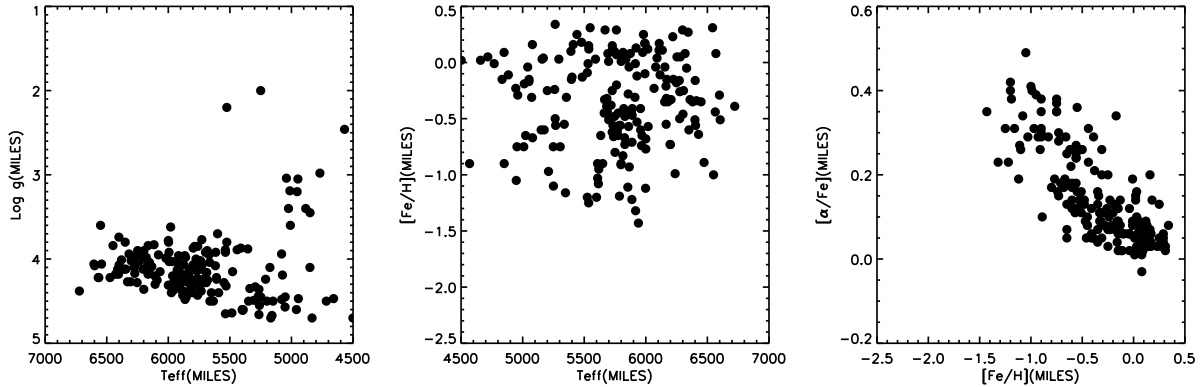

Fig. 7 Distribution of the MILES star sample in the planes of $T_{\rm eff} - \log g$, $T_{\rm eff}$ − [Fe/H] and [Fe/H] − [α/Fe].

spheric parameters and [α/Fe] span nearly the whole range of the parameter space associated with our synthetic spectra. Thus the result of the HRS sample can provide some limitations on our method in the range of parameter space.

Figure 11 shows the comparison between our [α/Fe] measurements and the determinations in the literature of high-resolution spectroscopic analysis. Figure 11 illustrates that there is an overall offset of −0.12 dex between our determinations and the values in the literature, along with a dispersion of 0.09 dex. Considering the zero-point offset of 0.13 dex with respect to our [α/Fe] measurements,

the LSP3 estimates are very consistent with the determinations derived from high-resolution spectral analysis as shown by the dashed line in the left panel of Figure 11.

Figure 12 shows the differences in [α/Fe] between the LSP3 measurements and the literature values along with the stellar atmospheric parameters. It demonstrates that the differences in [α/Fe] for the HRS sample have no significant correlations with $T_{\rm eff}$, $\log g$ or [Fe/H], except for being slightly lower for cold stars with $T_{\rm eff} < 5100$ K. Considering that the stellar atmospheric parameters of these HRS stars are also estimated by the LSP3, the slight
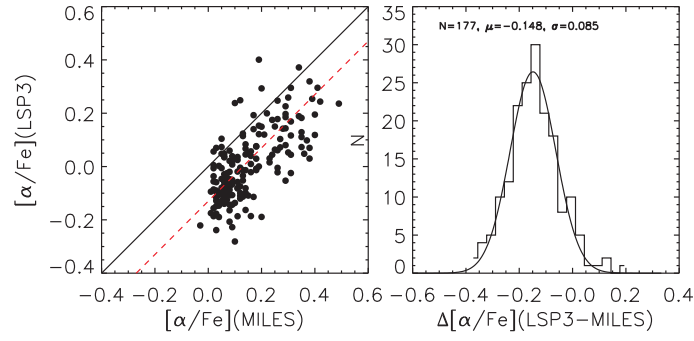
Fig. 8 Comparison of [α/Fe] between measurements of LSP3 and values from the literature for sample stars from the MILES library. "MILES" indicates the value of [α/Fe] from the literature of high-resolution spectroscopic analysis, while "LSP3" denotes our measurements. The left panel plots our measurements against the literature values. The solid and dashed lines show the true one-to-one correspondence and that after zero-point correction via an overall shift of 0.13 dex, respectively. The right panel is a Gaussian fit to the differences between our measurements and those from the literatures.
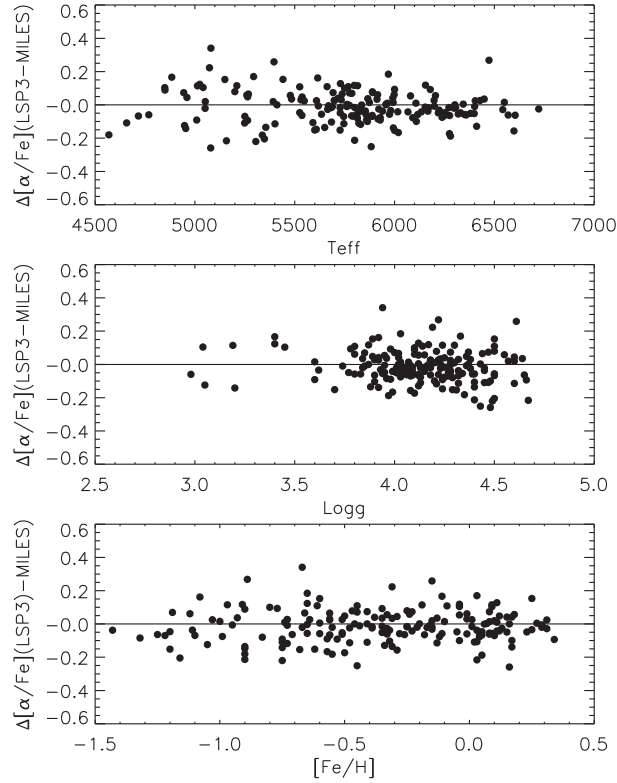
Fig. 9 The differences in [α/Fe] between the LSP3 measurements and the high-resolution values as functions of $T_{\rm eff}$ (*top*), $\log g$ (*middle*) and [Fe/H] (*bottom*), for the MILES stars.

trend in the differences means our measurements of [α/Fe] are systematically lower for the cold stars. Of course, we need to enlarge the number of stars in the HRS sample and the space of atmospheric parameters to determine the range where estimating [α/Fe] with the LSP3 is applicable.

4 UNCERTAINTIES IN [α/FE] MEASUREMENTS

The uncertainties in the [α/Fe] measurements include systematic errors and random errors, and the total error can be estimated as

$$\sigma_{\rm tot} = \sqrt{\sigma_{\rm sys}^2 + \sigma_{\rm ran}^2}, \tag{2}$$

where $\sigma_{\rm sys}$ represents the systematic errors, which are the inherent errors in the template-matching approach, and $\sigma_{\rm ran}$ represents the random errors, which are induced by the limited spectral quality and stellar parameters. Because the [α/Fe] measurements of our HRS sample are determined with the stellar atmospheric parameters obtained from LAMOST spectra by the LSP3, the results must include errors from both $\sigma_{\rm sys}$ and $\sigma_{\rm ran}$. Figure 11 illustrates that there is an overall offset of -0.12 dex between the LSP3 measurements and the values in the literature, along with a dispersion of 0.09 dex. Considering the zero-point offset of 0.13 dex for our measurements, such an offset of
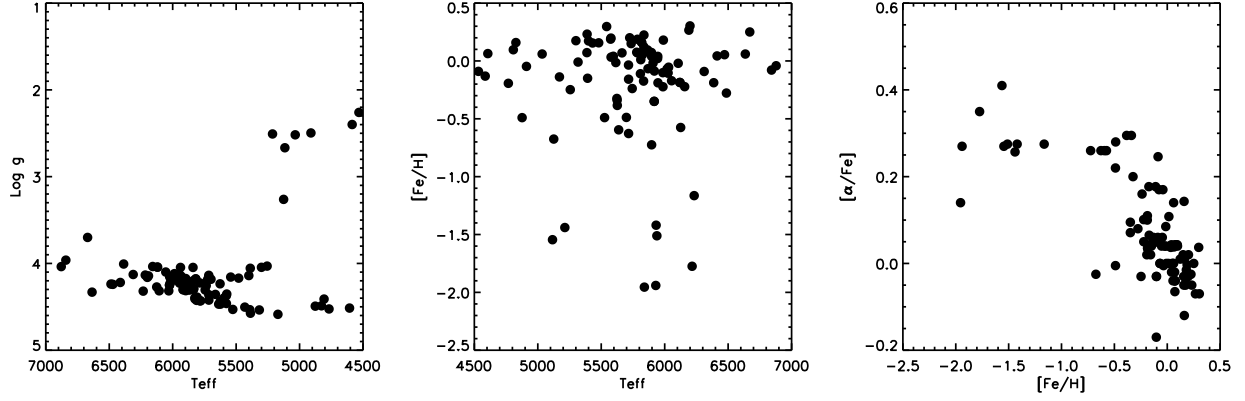
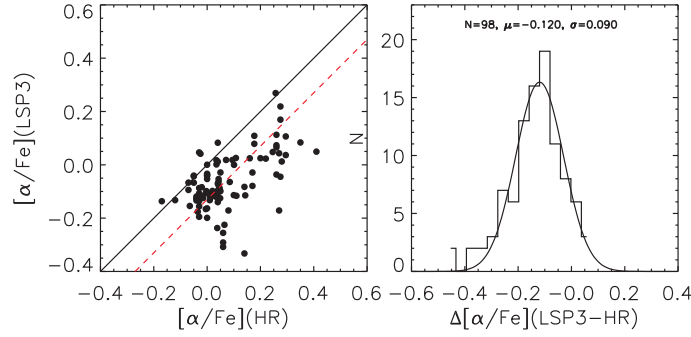**Fig. 10** The scatter diagram of $T_{\rm eff} - \log\ g$, $T_{\rm eff}$–[Fe/H] and [Fe/H]–[α/Fe] for the HRS sample stars.

Fig. 11 Comparison of [α/Fe] between measurements of the LSP3 and values from the literature for the HRS stars. The notation 'HR' denotes the determinations from high-resolution spectra, while 'LSP3' refers to our measurements from the LAMOST spectra. The solid and dashed lines in the left panel show the true one-to-one correspondence and that after zero-point correction via an overall shift of 0.13 dex, respectively. The right panel is a Gaussian fit to the differences between our measurements and those from the literature.

Table 1 List of the Atmospheric Parameters and the [α/Fe] Values for HRS

Star name	LAMOST ID	High-resolution					LSP3			
		$T_{\rm eff}$	$\log\ g$	[Fe/H]	[α/Fe]		$T_{\rm eff}$	$\log\ g$	[Fe/H]	[α/Fe]
HD000004	20111212-B90801-6-178	6779	3.87	0.21	0.00		6671	3.70	0.25	–0.16
HD079969	20111215-B91104-15-144	4825	4.40	–0.05	0.04		4606	4.51	0.06	–0.24
HD078234	20120113-B5594004-16-6	6703	3.87	–0.32	0.17		6878	4.04	–0.04	–0.03
HD097658	20120113-B5594006-8-178	5136	4.50	–0.32	0.05		5171	4.59	–0.14	–0.10
HD106510	20120113-B5594007-3-176	5802	4.50	–0.50	0.07		5917	4.30	–0.35	0.02
HD107611	20120123-B5595005-3-99	6425	4.38	–0.06	0.00		6413	4.22	0.04	–0.10
HD102080	20120126-B5595304-5-226	5979	4.27	–0.42	0.04		6121	4.04	–0.19	0.00
HD112887	20120126-B5595305-12-154	6319	3.88	–0.44	0.11		6386	4.01	–0.19	–0.12
HD107611	20120201-B5595905-3-99	6425	4.38	–0.06	0.00		6472	4.24	0.05	–0.05
...	...	...	...	...	...	...	...	...	...	...

Notes: This table is available in its entirety in machine-readable and Virtual Observatory (VO) formats in the online version of the journal (*www.raa-journal.org/docs/Supp/ms2760tab1.pdf*). A portion is shown here for guidance regarding its form and content.

−0.12 dex will disappear, while the standard deviation of 0.09 dex can be taken as the $\sigma_{\rm sys}$ between our measurements and values from high-resolution spectroscopic analysis.

The random errors result from the uncertainties in the stellar parameters and the quality of target spectra. Lee et al. (2011) determine random errors by adding artificial noise to the observed flux, but it is better to estimate the random errors using multiple observations of the same targets. The LAMOST survey provides a large number of repeated spectra due to overlapping of fields of view of adjacent plates. About 23% of stars that are targets in the LSS-GAC have been observed more than once (Liu et al. 2014), and these multi-epoch observations of the same targets are used to estimate the random errors in our [α/Fe] estimates. Owing to unstable atmospheric conditions, two-
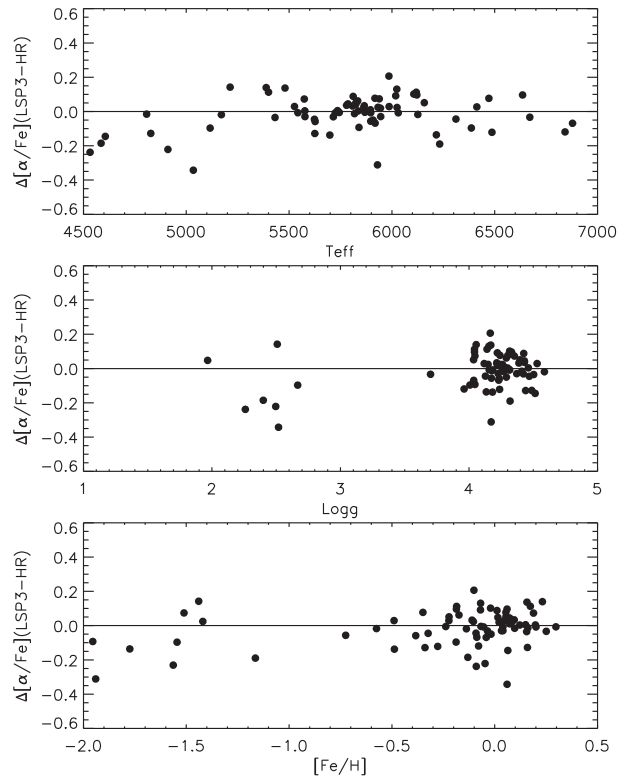
Fig. 12 The differences of [α/Fe] as a function of T_{eff} (*top*), $\log g$ (*middle*), and [Fe/H] (*bottom*) for the HRS stars.

epoch observations of the same target may have different SNRs. In order to obtain a more accurate estimation of the random errors, we employ targets with a difference in spectral SNRs of the repeated observations of less than 20%. As a result, 30 170 pairs of spectra with SNR > 15 for the repeated targets of the LSS-GAC are selected.

Figure 13 shows the distributions of stellar parameters of the sample stars with repeated observations in the planes of $T_{\mathrm{eff}} - \log g$ and $T_{\mathrm{eff}} - $ [Fe/H]. Figure 14 plots the differences in [α/Fe] between repeated observations along with the spectral SNRs, T_{eff}, $\log g$ and [Fe/H] from the upper to lower panels, respectively. It demonstrates that σ_{ran} decreases gradually from 0.09 to 0.01 dex with the increase of spectral SNRs from 20 to 200, but σ_{ran} has no clear correlation with the stellar atmospheric parameters. The abrupt increase in σ_{ran} at lower metallicity is just a false appearance due to the fewer number of very metal-poor stars. Thus, the random errors are mainly due to the spectral SNRs. In order to ensure the random error is not larger than the systematic error, we should limit spectral SNRs to be higher than 30.

5 DISCUSSION OF THE ERROR SOURCES

There are several factors that influence the determination of [α/Fe]. For instance, (1) uncertainties in the stellar atmospheric parameters, (2) SNRs of the target spectra, and (3) variation of the spectral resolution of the target spectra. Those factors act interactively rather than in isolation,

which makes accurate error estimation become very complex and difficult.

5.1 Uncertainty from Stellar Atmospheric Parameters

As listed in Table 1, we have two sets of atmospheric parameters for the HRS sample stars; one is determined from LAMOST spectra by the LSP3, and the other is from the literature of high-resolution spectroscopic analysis. Figure 15 plots the comparison of the two sets of atmospheric parameters. The HRS is a good sample to investigate the effects of stellar parameters on the [α/Fe] measurements. Therefore, we recalculated the [α/Fe] measurements of the HRS sample stars using the atmospheric parameters derived from high-resolution spectra. Figure 16 plots the differences of the two sets of [α/Fe] measurements along with differences in atmospheric parameters.

The left and middle panels of Figure 15 show that the two sets atmospheric parameters are consistent with each other for T_{eff} and $\log g$ within their error bars, but [Fe/H] was overestimated by the LSP3 with 0.06 dex higher than that from the literature on average as the right panel of Figure 15 demonstrates. This result is in good agreement with other comparisons presented by Xiang et al. (2015).

Figure 16 shows that the differences in [α/Fe] measurements determined with the two sets of atmospheric parameters have no correlation with the differences in atmospheric parameters. The mean difference in [α/Fe] is about −0.05 dex, which means that the uncertainty from atmospheric parameters on the [α/Fe] measurements is
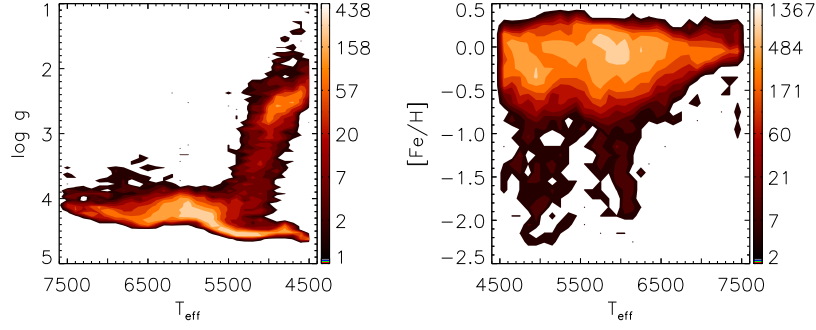
Fig. 13 Density distributions of the repeated observations of stars in the planes of $T_{\rm eff} - \log g$ and $T_{\rm eff} - $[Fe/H].
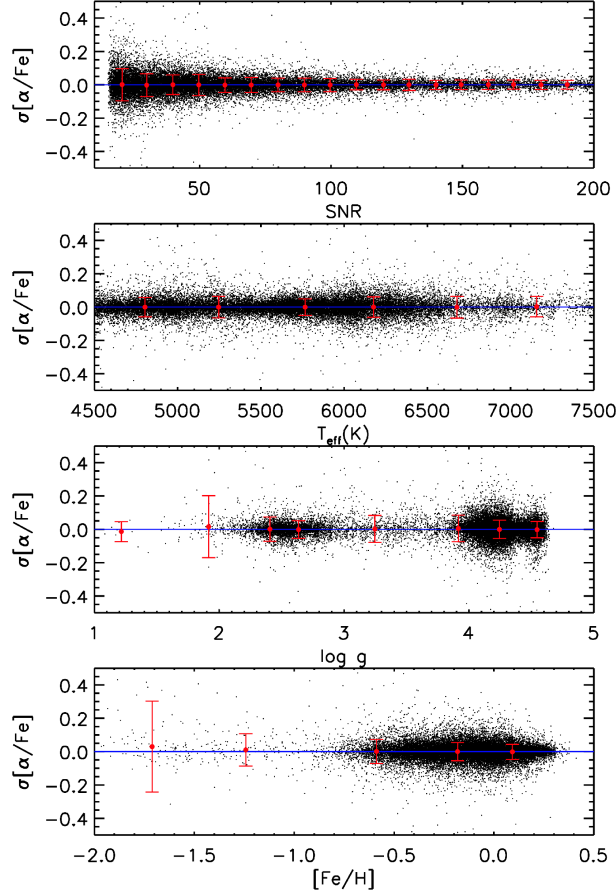

Fig. 14 The differences in [α/Fe] between repeated observations as a function of SNR, $T_{\rm eff}$, $\log g$ and [Fe/H]. The red dots and the error bars are the mean differences and dispersions in different bins respectively. The bin sizes are 10, 500 K, 0.5 dex and 0.5 dex from the upper to lower panels, respectively.

−0.05 dex, mainly due to the higher [Fe/H] determined by the LSP3.

5.2 Uncertainty from the Spectra

The quality of the spectra, including the spectral SNRs and resolution, is the key factor that determines the accuracy of [α/Fe] measurements. Figure 14 shows the uncertainties in [α/Fe] from the spectral SNRs. Here, we discuss the influence of spectral resolution. Due to the unique de-

sign of LAMOST, which acquires 4000 fiber spectra in a single exposure, the resolutions of the individual spectra are not uniform (Xiang et al. 2015). The resolution of the LAMOST spectra varies for different fibers, but in the process of template-matching we have fixed the resolution of the synthetic spectra to the average resolution (FWHM = 2.8 Å) for all 4000 fibers. How does the inconsistent resolution of observed and synthetic spectra influence the [α/Fe] measurements? We try to investigate this effect with spectra from the HRS sample.
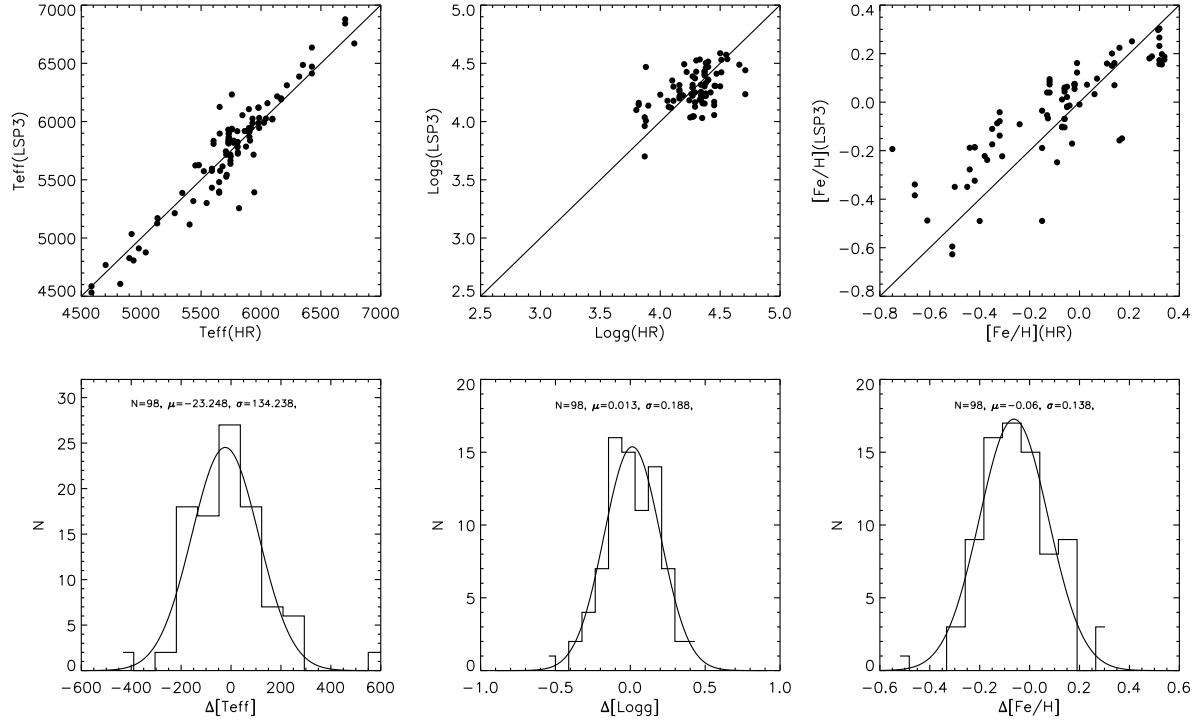
Fig. 15 Comparison of stellar atmospheric parameters for 98 HRS stars. The notation 'HRS' denotes high-resolution spectra, while 'LSP3' refers to LAMOST spectra.
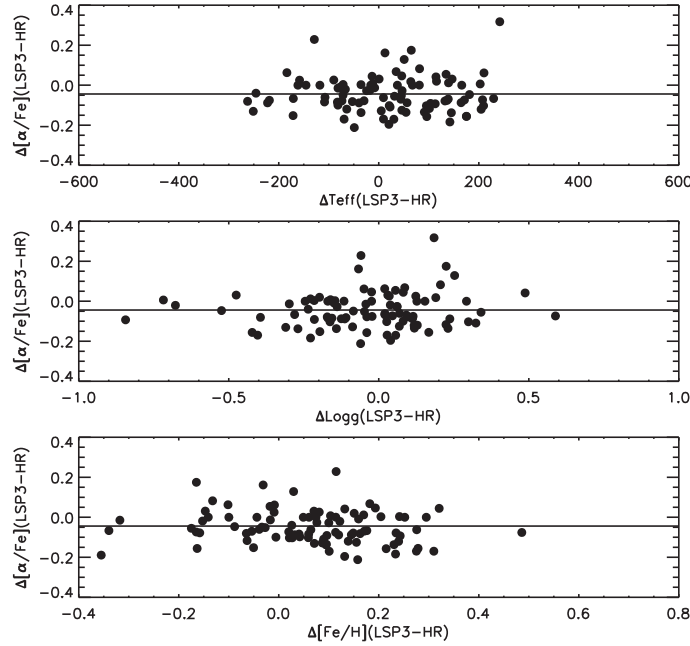

Fig. 16 Differences in [α/Fe] between the two sets of measurements with atmospheric parameters from LSP3 and those from the literature as a function of differences in T_{eff}, $\log g$ and [Fe/H], from top to bottom respectively.

First, we degrade the resolution of the observed spectra to the lowest limit of FWHM = 4 Å for LAMOST spectra, but the resolution of synthetic spectra is still FWHM = 2.8 Å. With the degraded HRS spectra, we recalculate the [α/Fe] for HRS stars by the LSP3. The left panel of

Figure 17 plots the differences in [α/Fe] between the new measurements from spectra with FWHM = 4 Å and the original values from spectra with FWHM = 2.8 Å along with [α/Fe] from high-resolution spectra. We note that, for most of the sample stars, the [α/Fe] measurements es-
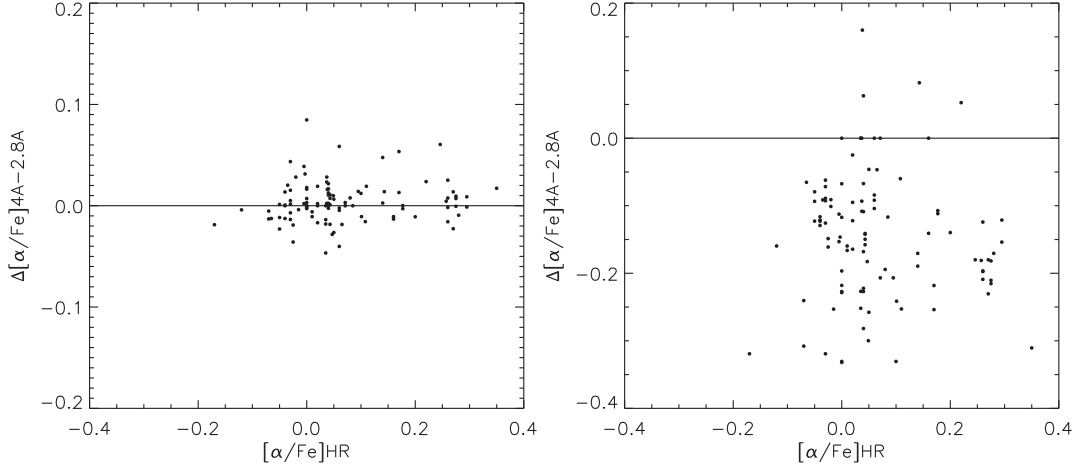
Fig. 17 Differences in [α/Fe] measurements for the HRS stars derived from the degraded LAMOST spectra (FWHM = 4 Å) and the original LAMOST spectra (FWHM = 2.8 Å) compared with the [α/Fe] values in the literature. The [α/Fe] measurements from the degraded spectra with FWHM = 4.0 Å were estimated with the synthetic template spectra with FWHM = 2.8 Å in the left panel, but they were estimated with the synthetic template spectra with FWHM = 4.0 Å in the right panel. The notation '2.8A' refers to the [α/Fe] measurements from the original LAMOST spectra, while the 'HR' denotes the high-resolution measurements from the literature.

timated from the degraded LAMOST spectra are much lower than the values estimated from original LAMOST spectra. The differences are out of the range of the total errors in our [α/Fe] measurements. This result indicates the nonuniform resolutions for the target and synthetic spectra will lead to some uncertainties in our [α/Fe] measurements. In fact, the true variation for the LAMOST spectral resolution is not so large in our selected wavelength range when measuring [α/Fe], therefore the true difference is much less than that present in this example.

Second, we degrade the resolution of both the observed and synthetic spectra to the same value of FWHM = 4.0 Å, and then measure the [α/Fe] ratios again. The right panel of Figure 17 plots the differences between the [α/Fe] measurements from the degraded spectra (FWHM = 4 Å) both for targets and synthetic templates and the measurements from primary LAMOST spectra (FWHM = 2.8 Å) along with the [α/Fe] values in the literature. It shows no systematic deviation between the two sets of [α/Fe] measurements. This result means the [α/Fe] measurements determined with different resolutions of observed spectra are in good agreement if we can ensure the observed and synthetic spectra have the same resolution.

6 SUMMARY

Using the template-matching technique of the LSP3 pipeline, we provide a method of measuring the [α/Fe] abundances from low-resolution spectra provided by the LAMOST survey. We do three tests to examine the validity of our method by employing sample stars from the ELODIE and MILES libraries, as well as the LAMOST survey. By comparing our [α/Fe] measurements with those from high-resolution spectroscopic analysis, we conclude that our method is capable of measuring [α/Fe] from LAMOST spectra. Based on the results for the sample

HRS from LAMOST spectra, we suggest that our method can give reliable [α/Fe] measurements for stars with stellar atmospheric parameters of $T_{\rm eff}$ = [5000, 7500] K, $\log g$ = [1.0, 5.0] dex and [Fe/H]=[−1.5, +0.5] dex. For cold ($T_{\rm eff} < 5000$ K) or metal-poor ([Fe/H]< −1.5) stars, the [α/Fe] measurements are systematically lower than values from high-resolution spectroscopic analysis. In addition, we find that there is an overall lower deviation of about −0.13 dex for our [α/Fe] measurements compared with values from high-resolution spectroscopic analysis in the literature. We need to enlarge the number of member stars in the HRS sample to further refine the systematic offset in [α/Fe] measurements and the space of atmospheric parameters suitable for our method.

The errors in our [α/Fe] measurements come from uncertainties in stellar atmospheric parameters, and the spectral SNR and resolution. To ensure the total error is less than 0.1 dex, the SNRs of the observed spectra should be higher than 20. The varying resolution of the LAMOST spectra is also a source of uncertainty in our [α/Fe] measurements. At present, the LAMOST public release does not contain information on how the spectral resolution varies with wavelength, fiber or time. In future work, we will incorporate day to day and fiber to fiber variations in analysis of the spectral resolution, and adjust the resolution of the synthetic spectra to match the observed spectra to reduce errors in [α/Fe] measurements.

References

Adibekyan, V. Z., Figueira, P., Santos, N. C., et al. 2013, A&A, 554, A44

Bensby, T., Feltzing, S., & Lundström, I. 2004, A&A, 421, 969

Bensby, T., Feltzing, S., & Oey, M. S. 2014, A&A, 562, A71

Boeche, C., Siebert, A., Williams, M., et al. 2011, AJ, 142, 193

Burbidge, E. M., Burbidge, G. R., Fowler, W. A., & Hoyle, F. 1957, Reviews of Modern Physics, 29, 547

Castelli, F., & Kurucz, R. L. 2004, astro-ph/0405087

Chen, Y. Q., Nissen, P. E., Zhao, G., Zhang, H. W., & Benoni, T. 2000, A&AS, 141, 491

Deng, L.-C., Newberg, H. J., Liu, C., et al. 2012, RAA (Research in Astronomy and Astrophysics), 12, 735

Edvardsson, B., Andersen, J., Gustafsson, B., et al. 1993, A&A, 275, 101

Falcón-Barroso, J., Sánchez-Blázquez, P., Vazdekis, A., et al. 2011, A&A, 532, A95

Franchini, M., Morossi, C., Di Marcantonio, P., Malagnini, M. L., & Chavez, M. 2010, ApJ, 719, 240

Franchini, M., Morossi, C., Di Marcantonio, P., Malagnini, M. L., & Chavez, M. 2011, ApJ, 730, 117

Fuhrmann, K. 2004, Astronomische Nachrichten, 325, 3

Fulbright, J. P. 2002, AJ, 123, 404

Gratton, R. G., Carretta, E., Desidera, S., et al. 2003, A&A, 406, 131

Grevesse, N., & Sauval, A. J. 1998, Space Sci. Rev., 85, 161

Hinkel, N. R., Timmes, F. X., Young, P. A., Pagano, M. D., & Turnbull, M. C. 2014, AJ, 148, 54

Lee, Y. S., Beers, T. C., Sivarani, T., et al. 2008, AJ, 136, 2022

Lee, Y. S., Beers, T. C., Allende Prieto, C., et al. 2011, AJ, 141, 90

Lee, Y. S., Beers, T. C., Masseron, T., et al. 2013, AJ, 146, 132

Liu, X.-W., Yuan, H.-B., Huo, Z.-Y., et al. 2014, in IAU Symposium, 298, Setting the Scene for Gaia and LAMOST, eds. S. Feltzing, G. Zhao, N. A. Walton, & P. Whitelock, 310

Luo, A.-L., Zhao, Y.-H., Zhao, G., et al. 2015, RAA (Research in Astronomy and Astrophysics), 15, 1095

McWilliam, A. 1997, ARA&A, 35, 503

Moultaka, J., Ilovaisky, S. A., Prugniel, P., & Soubiran, C. 2004, PASP, 116, 693

Nissen, P. E., & Schuster, W. J. 2010, A&A, 511, L10

Prugniel, P., Soubiran, C., Koleva, M., & Le Borgne, D. 2007, astro-ph/0703658

Reddy, B. E., Lambert, D. L., & Allende Prieto, C. 2006, MNRAS, 367, 1329

Sánchez-Blázquez, P., Peletier, R. F., Jiménez-Vicente, J., et al. 2006, MNRAS, 371, 703

Soubiran, C., & Girard, P. 2005, A&A, 438, 139

Soubiran, C., Le Campion, J.-F., Cayrel de Strobel, G., & Caillo, A. 2010, A&A, 515, A111

Steinmetz, M., Zwitter, T., Siebert, A., et al. 2006, AJ, 132, 1645

Tinsley, B. M. 1979, ApJ, 229, 1046

Wu, Y., Luo, A.-L., Li, H.-N., et al. 2011, RAA (Research in Astronomy and Astrophysics), 11, 924

Xiang, M. S., Liu, X. W., Yuan, H. B., et al. 2015, MNRAS, 448, 822

Yanny, B., Rockosi, C., Newberg, H. J., et al. 2009, AJ, 137, 4377

Yuan, H.-B., Liu, X.-W., Huo, Z.-Y., et al. 2015, MNRAS, 448, 855

Zhang, H. W., & Zhao, G. 2006, A&A, 449, 127

Zhao, G., Zhao, Y.-H., Chu, Y.-Q., Jing, Y.-P., & Deng, L.-C. 2012, RAA (Research in Astronomy and Astrophysics), 12, 723